Molecular Neurobiology (2019) 56:844–856
https://doi.org/10.1007/s12035-018-1129-2

The Pharmacological Inhibition of Fatty Acid Amide Hydrolase Prevents Excitotoxic Damage in the Rat Striatum: Possible Involvement of CB1 Receptors Regulation

Gabriela Aguilera-Portillo[1,2] · Edgar Rangel-López[1] · Juana Villeda-Hernández[3] · Anahí Chavarría[4] · Pilar Castellanos[5] · Zubeyir Elmazoglu[6] · Çimen Karasu[6] · Isaac Túnez[7] · Gibrán Pedraza[8] · Mina Königsberg[8] · Abel Santamaría[1]

Received: 6 March 2018 / Accepted: 14 May 2018 / Published online: 25 May 2018

Abstract

The endocannabinoid system (ECS) actively participates in several physiological processes within the central nervous system. Among such, its involvement in the downregulation of the N-methyl-D-aspartate receptor (NMDAr) through a modulatory input at the cannabinoid receptors (CBr) has been established. After its production via the kynurenine pathway (KP), quinolinic acid (QUIN) can act as an excitotoxin through the selective overactivation of NMDAr, thus participating in the onset and development of neurological disorders. In this work, we evaluated whether the pharmacological inhibition of fatty acid amide hydrolase (FAAH) by URB597, and the consequent increase in the endogenous levels of anandamide, can prevent the excitotoxic damage induced by QUIN. URB597 (0.3 mg/kg/day × 7 days, administered before, during and after the striatal lesion) exerted protective effects on the QUIN-induced motor (asymmetric behavior) and biochemical (lipid peroxidation and protein carbonylation) alterations in rats. URB597 also preserved the structural integrity of the striatum and prevented the neuronal loss (assessed as microtubule-associated protein-2 and glutamate decarboxylase localization) induced by QUIN (1 μL intrastriatal, 240 nmol/μL), while modified the early localization patterns of CBr1 (CB1) and NMDAr subunit 1 (NR1). Altogether, these findings support the concept that the pharmacological manipulation of the endocannabinoid system plays a neuroprotective role against excitotoxic insults in the central nervous system.

Keywords Endocannabinoid system · Fatty acid amide hydrolase · Cannabinoid receptor agonists · Neuroprotection · Excitotoxicity · Oxidative stress

Introduction

Oxidative stress, inflammation, mitochondrial energy depletion, and excitotoxicity, constitute confluent events intimately related to neuronal cell death via activation of apoptotic/necrotic pathways [1]. Characteristic hallmarks of excitotoxicity include increased intracellular calcium recruitment as a consequence of the persistent opening of ion

✉ Abel Santamaría
absada@yahoo.com

[1] Laboratorio de Aminoácidos Excitadores, Instituto Nacional de Neurología y Neurocirugía Manuel Velasco Suárez, Insurgentes Sur 3877, 14269 Mexico, Mexico

[2] Posgrado en Biología Experimental, DCBS, Universidad Autónoma Metropolitana-Iztapalapa, 09310 Mexico, Mexico

[3] Laboratorio de Patología Experimental, Instituto Nacional de Neurología y Neurocirugía, 14269 Mexico, Mexico

[4] Unidad de Investigación en Medicina Experimental, Facultad de Medicina, Universidad Nacional Autónoma de México, 04510 Mexico, Mexico

[5] Departamento de Ingeniería Eléctrica, División de Ciencias Biológicas y de la Salud, Universidad Autónoma Metropolitana-Iztapalapa, 09310 Mexico, Mexico

[6] Cellular Stress Response and Signal Transduction Research Laboratory, Faculty of Medicine, Department of Medical Pharmacology, Gazi University, Beşevler, 06500 Ankara, Turkey

[7] Instituto Maimonides de Investigación Biomédica de Córdoba (IMIBIC) & Departmento de Bioquímica y Biología Molecular, Facultad de Medicina y Enfermería, Universidad de Córdoba, Cordoba, Spain

[8] Departamento de Ciencias de la Salud, División de Ciencias Biológicas y de la Salud, Universidad Autónoma Metropolitana-Iztapalapa, 09310 Mexico, Mexico

calcium channels associated to N-methyl-D-aspartate (NMDA) receptors (NMDAr); an event described thoroughly in previous publications [1–3]. Such changes are responsible for the activation of various well-known metabolic pathways that elicit deleterious effects, leading to the increased formation of reactive oxygen and nitrogen species (ROS/RNS); inflammatory responses; persistent activation of degrading enzymes (endonucleases, proteases, etc.); mitochondrial dysfunction; and cell death [4].

The neuroactive properties of metabolites from the kynurenine pathway (KP), such as kynurenic acid (KYNA, generated in the side chain of the pathway), and those with neurotoxic profiles, like 3-hydroxy-anthranilic acid (3-OH-AA) [5], have pointed out to the KP as a metabolic route of major significance given the excitatory/inhibitory responses exerted by these compounds, as well as the fact that this pathway leads to the synthesis of the active molecule NAD^+ as the final product [6]. Besides its role as a transitory metabolite of the KP, quinolinic acid (QUIN, or 2,3-pyridine dicarboxylic acid) constitutes a selective endogenous glutamate agonist. Several reports have consolidated QUIN as a valid and useful experimental tool to induce both excitotoxicity and oxidative stress under in vitro and in vivo conditions [7–9]. More importantly, QUIN acts with high specificity on selective populations of NMDAr, a condition that may help to explain the selectivity of the toxic actions of this metabolite in the brain. The underlying toxic mechanism triggered by QUIN involves an intracellular enhancement of Ca^{2+} levels paralleled an extracellular increase in glutamate levels, the reduced activity of antioxidant systems, and a consequent increase in ROS/RNS formation, all resulting in energy depletion, oxidative stress, and cell death [10–12].

The cannabinoid receptors (CBr) belong to the Gi/o family of receptors characterized for its seven transmembrane domains. Two subtypes have been described: the CB1 and CB2 receptors; while these receptors are present both peripherally and within the central nervous system (CNS), a differential distribution occurs [13]. CB1 are considered one of the most abundant G protein-coupled receptors in the CNS and expressed with high density in basal ganglia, neocortex, hippocampus, and cerebellum [14], where they modulate glutamate release and regulate the inhibition of adenylate cyclase after their activation [15, 16]. On the other hand, CB2 are mainly associated to immune cells and tissues; among many different roles, these receptors exhibit a modulatory effect on microglial function and regulate cytokine release in the CNS [14, 15].

Several endocannabinoids are known today, being anandamide (N-arachidonoylethanolamine or AEA; see Fig. 1) the most abundant of them. This molecule binds to CB1 and CB2 with high affinity; then, the receptor activation turns readily into an intracellular hydrolysis of AEA to ethanolamine and arachidonic acid catalyzed by the enzyme fatty acid amide hydrolase (FAAH; EC 3.5.1.99) [17, 18]. In turn, synthetic cannabinoids act upon CB1, CB2, or both; for example, (*R*)-(+)-[2,3-dihydro-5-methyl-3-(4-morpholinylmethyl)pyrrolo[1,2,3-*de*]-1,4-benzoxazin-6-yl]-1-naphthalenylmethanone mesylate (WIN 55,212–2) mostly binds to CB1, whereas 4-[4-(1,1-dimethylheptyl)-2,6-dimethoxyphenyl]-6,6-dimethylbicyclo[3.1.1]hept-2-ene-2-methanol (HU 308) has a higher affinity for CB2 [19]. Alternatively, tools such as [3-(3-carbamoylphenyl)phenyl]N-cyclohexylcarbamate (URB597; see Fig. 1) exhibit unique therapeutic potential and are increasingly incorporated into several experimental designs. As mentioned above, the biological activity of AEA in both the CNS and periphery is concluded just after its removal from the extracellular milieu through cellular uptake and protein transporters before an enzymatic degradation process occurs [20, 21]. Therefore, the selective inhibitor of the FAAH and URB597 can increase the intracellular levels of AEA, and its use has been associated with protective actions under different toxic scenarios in which it prevents cell death and reduces oxidative damage to biomolecules [22, 23]. Despite the mechanisms underlying these protective events remain unsolved, some hypotheses have been proposed in this regard. First, the excitation of postsynaptic neurons causes depolarization and the consequent influx of Ca^{2+}; the elevated Ca^{2+} levels stimulate the synthesis and release of different endocannabinoids, which later will bind to CBr on the presynaptic neuron; then, the activated CBr reduces the release of neurotransmitters [24]. Some other reports have

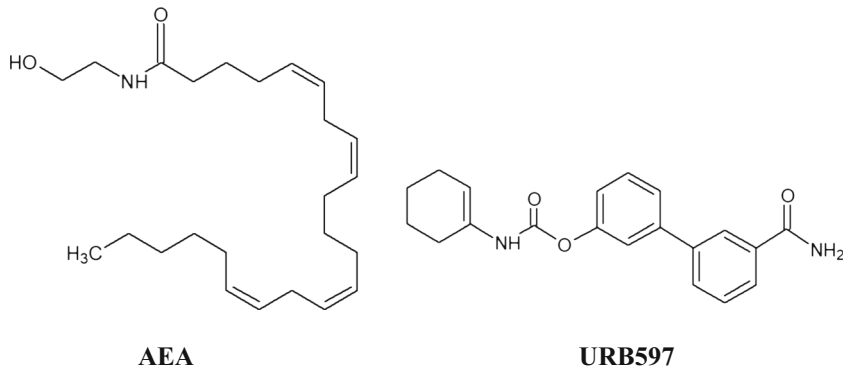

Fig. 1 Chemical structures of anandamide (AEA) and URB597. ACD/ChemSketch, 2017

shown that CB1 couples to NR1 subunits of the NMDAr via histidine triad nucleotide-binding protein 1 (HINT-1); then, a subsequent co-internalization process elicited by the presence of CBr agonists reduces the number of functional NMDAr, consequently blocking excitatory responses through a decrease in glutamatergic overactivation [25–27]. Also, some interactions of cannabinoids and nuclear elements have been recently suggested; while some studies have shown that cannabinoids (of synthetic or endogenous nature) can bind directly to peroxisome proliferator-activated receptors (PPARs) to change target gene expression, others have stated that metabolized cannabinoids might be active at PPARs [28, 29], or that cannabinoids might act at cell surface receptors that could trigger intracellular signaling cascades that render the activation of PPARs. In any case, all routes contribute to the anti-inflammatory effects of cannabinoids at the PPARs.

Numerous publications have recently demonstrated that the endocannabinoid system (ECS) is responsible for the reduction of NMDAr overactivation and the consequent cell protection against excitotoxic damage [26]. Hence, this mechanism substantiates novel approaches aiming to enhance or stimulate the ECS as a therapeutic strategy, including the avoidance of the toxic effects evoked by QUIN. Therefore, in this work, we evaluated whether the use of URB597 holds potential to prevent the deleterious effects (oxidative stress, cell damage, and motor alterations) induced by excitotoxic events in the rat striatum. For this purpose, we employed the in vivo toxic model produced by the intrastriatal injection of QUIN to rats, and just before different striatal tissue preparations were used to assess biochemical and morphological alterations, circling behavior was estimated in all animals as an index of motor disturbances. This model was used to assess the prophylactic potential of URB597 to reduce the harmful effects produced by QUIN via the ECS stimulation. Our results support a protective role of the ECS stimulation against excitotoxic insults.

Materials and Methods

Chemicals

All reagents were of analytical grade. URB597 was purchased to Cayman Chemical Co. (Ann Arbor, MI, USA). Apomorphine, QUIN, and thiobarbituric acid (TBA) were obtained from Sigma Chemical Co. (St, Louis, MO, USA). Anti-GAD65 (monoclonal) and anti-MAP-2 (polyclonal) antibodies were also obtained from Sigma Chemical Co. Polyclonal anti-NMDAR1 (NR1) and anti-CB1 antibodies were purchased to Abcam (Cambridge, UK). All required solutions were prepared using deionized water from a Milli-RQ system (Millipore, MA). All other chemicals were obtained from well-known commercial sources.

Animals

Adult male Wistar rats (280–320 g; $N = 72$) were used throughout the study. All animals were obtained from the vivarium of the Universidad Autónoma Metropolitana-Iztapalapa (UAM-I), Mexico. Rats were distributed six per cage and received standard rodent diet and water ad libitum. Additionally, animals were synchronized with 12:12 light-dark cycles, under standard temperature conditions (25 ± 1 °C), and 50% relative humidity. All procedures with animals were strictly developed to comply with the local guidelines for the use and care of laboratory animals (Norma Oficial Mexicana NOM-062-ZOO-2001), and the "Guidelines for the Use of Animals in Neuroscience Research" from the Society of Neuroscience. All experiments performed were timely approved by the Ethics Committee of the Instituto Nacional de Neurología y Neurocirugía. All efforts were made to minimize animal suffering during the experiments.

Experimental Design and Drug Infusion

This study encompassed four experimental groups ($N = 4$–6 per group). Rats were randomly assigned to one of these groups: (a) Sham group (intraperitoneal vehicle containing 5% Tween 80 + 10% DMSO 50 mM + 85% saline given on days 1 to 7, plus intrastriatal unilateral saline (1 μL) on day 4, 1 h after vehicle administration); (b) QUIN group (intraperitoneal vehicle on days 1 to 7, and intrastriatal unilateral QUIN (1 μL, 240 nmol/μL) on day 4, 1 h after vehicle administration); (c) URB597 group (intraperitoneal URB597 solution containing 0.3 mg/kg of URB + 0.5 mL of vehicle given on days 1 to 7, and intrastriatal unilateral saline (1 μL) on day 4, 1 h after vehicle administration); and (d) URB597 + QUIN group (intraperitoneal URB597 solution on days 1 to 7, and intrastriatal unilateral QUIN on day 4, 1 h after vehicle administration). Dosages and schemes of administration for QUIN and URB597 were chosen according to previous reports [22, 30, 31]. URB597 was administered before, during, and after the QUIN infusion to create a protective scenario around the striatal lesion. Animals from the different experimental groups were euthanized at three distinct times, depending on the nature of the test to which they were assigned: 8 days post-surgery for the histological and immunofluorescence assays (to assess striatal degeneration), 24 h post-surgery for the biochemical assays (to assess a causal role of oxidative stress in further cell degeneration), and 1.5 h post-surgery for additional immunofluorescence assays (to assess early protein regulation and localization as a mechanistic component of toxicity or protection). Therefore, the experiments were carried out from longer to shorter times to first assess tissue degeneration and/or preservation (8 days post-surgery), and later the possible causal nature of these events (24 and 1.5 h post-surgery).

Stereotaxic Surgery

Prior to the surgical procedures, rats were fully anesthetized (0.2 U per 250 g sodium pentobarbital, i.p.) and placed into a stereotaxic apparatus (Stoelting Co., IL). Using a rat brain atlas, vehicle or toxin were injected into the right striatum at a rate of 0.5 μL/1 min, using a 10 μL Hamilton microsyringe, at the following coordinates: AP = + 0.5 mm, L = − 2.6 mm, DV = − 4.5 mm [32]. After the infusion, the needle was left in place for 2 min before retraction. After surgery, animals were placed individually into clean cages until fully recovered.

Circling Behavior Test

Lesioned rats were evaluated by the circling behavior test after 5 min of receiving apomorphine hydrochloride (1 mg/kg), and for 60 min, on day 7 after surgery. This endpoint was tested to assess the degree of motor alterations due to striatal tissue degeneration. It is known that, following the unilateral intrastriatal injection of QUIN, animals exhibit turning behavior in response to the dopamine (DA) agonist apomorphine. This method is based on the fact that the striatal degeneration compromises DA transmission, which exerts a tonic influence on the striatal neurons; thus, drugs altering dopaminergic transmission also modulate locomotor activity [33]. The number of rotations ipsilateral to the lesioned hemisphere were counted and compared between groups. No rotations contralateral to the lesioned hemisphere were observed in animals in this study.

Histological Assessment

A representative number of animals from all groups was transcardially perfused on day 8 post-surgery with paraformaldehyde 4%. Whole brains were collected and paraffin-embedded to obtain coronal sections (5-μm thick) with a Leica RM2255 microtome (Leica Geosystems AD, St. Gallen, Switzerland). Sections were dewaxed and rehydrated. Further, hematoxylin & eosin staining was used for the histological analysis of the striatum. Digital images (×40) were obtained in a Nikon ECLIPSE E200 microscope (DiaMedical USA, West Bloomfield, MI), using the Q-capture Pro 7 software. Also, the ratio of cell damage was calculated by counting the number of damaged cell nuclei vs. the total number of cells per field in triplicate.

Immunofluorescence Assay for Microtubule-Associated Protein-2, Glutamate Decarboxylase, CB1, and NR1 Localization in the Striatum

Immunofluorescence assays were carried out in coronal brain sections at the striatal (dorsal area) level from the paraffin blocks obtained from rats of all groups. All sections were incubated with the primary antibodies to identify and localize CB1 (Abcam ab3558), NR1 (Abcam ab17345), microtubule-associated protein-2 (MAP-2) (Sigma M3696) and glutamate decarboxylase (GAD) (Sigma SAB4200232). For CB1 and NR1, brains were processed at 1.5 h post-surgery to identify early changes in the expression of these proteins; in contrast, MAP-2 and GAD staining was performed in sections obtained from rat brains at 8 days post-surgery to evidence neuronal cell loss. Brain sections were dewaxed and timely rehydrated through decreasing ethanol solutions. Antigens were unmasked with citrate buffer (0.1 M monohydrated citric acid/0.1 M dehydrated trisodium citrate). Sections were then blocked with universal blockade solution (Biogenex, Fremont, CA). After washing with Triton X-100 (0.2% in PBS, pH 7.2) for 30 min, sections were incubated overnight (4ºC) with the corresponding antibodies (anti-CB1, anti-NR1, anti-GAD, or anti-MAP-2, all at a 1:200 dilution). Slides were then incubated with 0.6 M glycine for 20 min to remove autofluorescence of aldehydes, and further washed three times with 0.5% PBS-albumin (PBA). The anti-rabbit coupled Alexa-488 (Thermo Fisher, Waltham, MA) and anti-mouse-coupled rhodamine (Santa Cruz Biotechnology, Santa Cruz, CA) secondary antibodies were diluted (1:2000) and incubated for 60 min at room temperature. Slides were then washed three times with PBS (pH 7.2). Nuclei were stained in blue with DAPI (Santa Cruz Biotechnology, Santa Cruz, CA), and sections were mounted with a fluorescent solution (DakoCytomation, Glostrup, Denmark). Images (×20) were obtained in an LSM-780 NLO Confocal Microscope (Carl Zeiss, Germany), using a laser diode at 405 nm for DAPI, and an Ar/ML 458/488/514 nm laser for Alexa 488 and rhodamine fluorophores. For the analysis of images, the ZEN 2010 6.0 software (Carl Zeiss, Germany) was used. In addition, the Otsu's method (segmentation algorithm) was used to contrast merged cells positive to CB1, NR1, GAD, or MAP-2 proteins, according to a previous report [34]. The area was represented as relative intensity units different to the background in a binary image. The intensity of fluorescence was calculated using Matlab software (version 7.10.0, MATLAB. Natick, Massachusetts: The MathWorks Inc., Natick, Massachusetts, USA, 2010).

Lipid Peroxidation Assay

In tissue homogenates from the dorsal striatum obtained 24 h post-surgery, lipid peroxidation was estimated as the formation of thiobarbituric acid-reactive substances (TBARS), following a standardized protocol [35]. Aliquots of the homogenates (50 μL) were added to 100 μL of the TBA reagent (0.75 g of TBA + 15 g of trichloroacetic acid + 2.54 mL of HCl 1 N) and then incubated at 96 °C for 20 min. Samples were centrifuged at 12,000 rpm for 10 min at 4 °C. The

optical density of supernatants was estimated at 532 nm in a Cytation 3 Image Reader (BioTek). Results were calculated as nanomoles of TBARS per milligram protein by the previous interpolation of absorbance in a constructed standard curve of tetramethoxypropane (TMPO) and expressed as percent of peroxidation against Sham group.

Protein Carbonylation Assay

In tissue homogenates from the dorsal striatum obtained 24 h after the intrastriatal administration of the toxin (or vehicle), protein carbonylation was estimated as an index of oxidative damage to proteins, following a standardized protocol [31]. A total of 50 μL of streptomycin sulfate (10 mg of streptomycin sulfate/100 mL distilled water) were added to the homogenates (250 μL) the night before the experiment. Then, each sample was vigorously vortexed and centrifuged at 5000 rpm and 4 °C for 10 min. Pellets were discarded, and supernatants were added to 300 μL of dinitrophenylhydrazine (DNPH) (0.05 g DNPH/25 mL HCl 2.5 N); samples were left at room temperature and under dark for an hour. A total of 300 μL of trichloroacetic acid (TCA) 20% was subsequently added and vortexed, and samples were placed in the freezer for 10 min; pellets were resuspended, and samples were centrifuged at 5000 rpm and 4 °C for 10 min. Supernatants were discarded and pellets were resuspended in 300 μL of TCA 10% and centrifuged at 5000 rpm and 4 °C for 10 min; this last step was done three times, and the samples were obtained clear and without yellow DNPH traces. The optical density of supernatants was estimated at 280 and 370 nm in a Cytation 3 Image Reader (Biotek). Results were calculated and expressed as nanomoles of DNPH per milligram of protein by the previous interpolation of absorbance in a constructed standard curve of DNPH.

Statistical Analysis

Results were expressed as mean values ± one standard error (SEM). Data were statistically analyzed by two-way analysis of variance (ANOVA), followed by Tukey's test. Values of $P < 0.05$ were considered of statistical significance. The statistical analysis was performed using the scientific statistic software GraphPad Prism 5 (GraphPad Scientific, San Diego, CA, USA).

Results

URB597 Prevented the QUIN-induced Body Weight Decrease

As a standard practice, the body weight of all animals was recorded every day prior to each drug administration. As seen in Fig. 2 (left panel), animals lesioned unilaterally with QUIN exhibited a significant decrease in body weight along the 12 days of experimentation compared to the Sham group (20% below Sham; $P < 0.05$). In contrast, animals lesioned with QUIN that also received URB597 exhibited a body weight gain similar to the Sham group (3% above Sham and 82% above the QUIN group; $P < 0.05$). URB597 per se did not affect body weight gain compared to the Sham group.

URB597 Attenuated the QUIN-induced Motor Asymmetry

We further evaluated whether the administration of URB597 (as pretreatment for 3 days, before the toxin administration, and as follow-up treatment for 3 days) could prevent or reduce motor asymmetry in animals lesioned unilaterally with QUIN. Results of this behavioral test are represented in the right panel

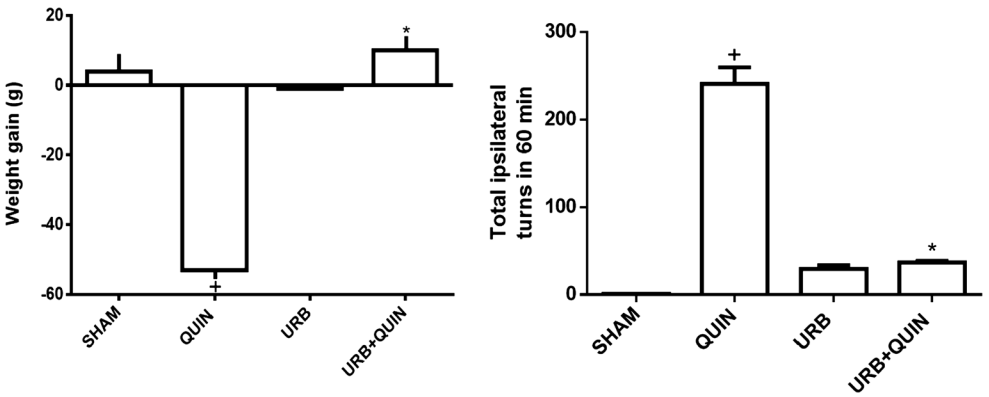

Fig. 2 Effects of quinolinic acid (QUIN) and/or URB597 (URB) on body weight changes and motor alterations in rats. The left panel depicts the overall weight gain of animals (initial weight of 280–320 g) exposed to QUIN and/or URB in 12 days. The right panel shows the total number of ipsilateral turns induced after apomorphine administration (1 mg/kg, s.c.) during 60 min in animals exposed to QUIN and/or URB. Mean values ± SEM of $N = 4–6$ rats per group are represented. $^{+}P < 0.05$, different from Sham; $^{*}P < 0.05$, different from QUIN; two-way ANOVA followed by Tukey's test

of Fig. 2. The group of animals with the QUIN-induced striatal lesion exhibited a significant motor asymmetry compared with the Sham group (230% above Sham; $P < 0.05$), and this effect was prevented by URB597 (89% below the QUIN group; $P < 0.05$), almost reaching control levels. URB597 per se did not affect rotation behavior compared to the Sham group.

URB597 Decreased the Striatal Cell Damage Induced by QUIN

Sections of dorsal striatum stained with hematoxylin and eosin evidenced that QUIN produced severe damage along the neuropil, pyknosis, and induced a higher number of damaged cell nuclei (Fig. 3, left panel, subset B) compared to the Sham group (left panel, subset A). In contrast, URB597 exerted effective protection of the striatal tissue of rats lesioned by QUIN (left panel, subset D), as evidenced by a preserved number of cell nuclei, neuropil, and striosomes. URB597 per se (left panel, subset C) did not affect the striatal structural integrity compared to the Sham group.

The assessment of the overall ratio of cell damage (no. of damaged cells/no. of total cells per field) is depicted in Fig. 3 (right panel). QUIN significantly increased the ratio of cell damage compared to the Sham group (117% above Sham; $P < 0.05$), and this effect was partially prevented by URB597 in QUIN-lesioned rats (27% below the QUIN group). URB597 per se did not affect the ratio of cell damage compared to the Sham group.

URB597 Attenuated the QUIN-induced Neuronal Loss of GABAergic GAD and MAP-2 Proteins in the Striatum

The immunofluorescence labeling (expression and localization) of the MAP-2 and GAD proteins was evaluated in striatal tissue sections obtained on day eight post-lesion as indexes of the levels of neuronal (GABAergic) cell loss and/or preservation (Fig. 4). While the left upper panels depict representative images (×20) of cell nuclei (stained with DAPI in blue) merged with GAD (in green), the left bottom panels show images (×20) of nuclei (again in blue) merged with MAP-2 (in red). For both proteins, the Sham and URB597 groups showed intense fluorescence labeling mostly located at the striosome level, and sometimes surrounding nuclei (upper and bottom panels). In contrast, the QUIN-lesioned tissue depicts diffuse and less intense green and red labelings, whereas the fluorescence intensities were partially recovered in the URB597 + QUIN treatment. The panels in the middle show the images contrasted by the segmentation procedure. Intense contrast is shown in the Sham and URB597 groups, whereas reduced contrast is shown in the QUIN group. This contrast was partially recovered for both proteins in the URB597 + QUIN group. The right panels depict the densitometric analysis (normalized) of the images, calculated after the segmentation procedure. The GAD and MAP-2 protein expression levels were reduced by QUIN by 48 and 60% compared to the Sham group, respectively, whereas URB597 prevented this effect (27% below and 48% above the Sham group, respectively). URB597 per se did not modify the expression

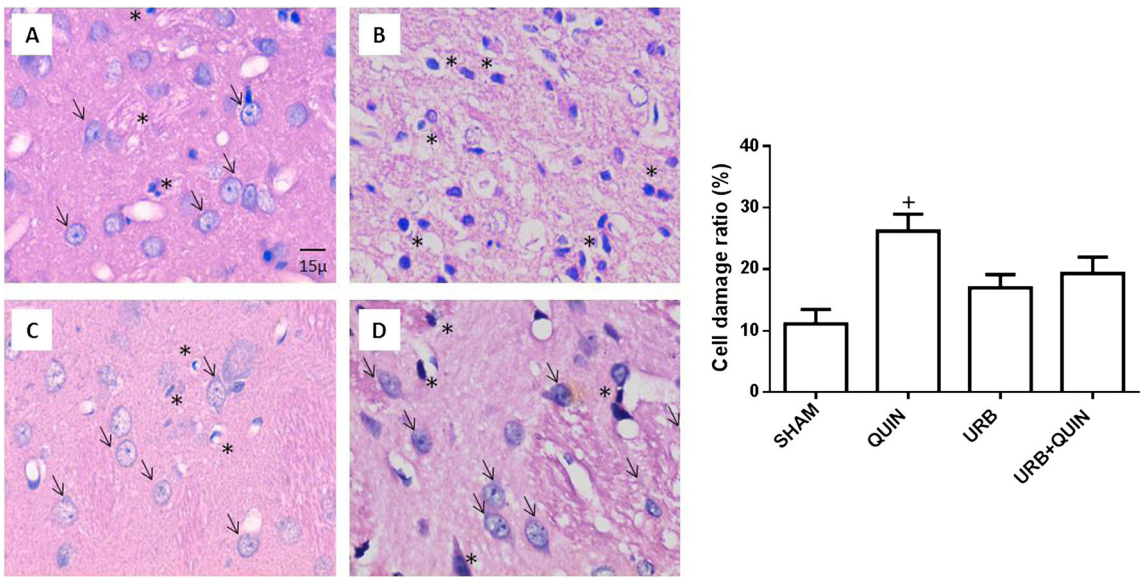

Fig. 3 Effects of quinolinic acid (QUIN) and/or URB597 (URB) on the striatal morphology in rats. The left panel shows photomicrographs (×40) of dorsal striatal tissue of animals exposed to QUIN and/or URB. **a** Sham. **b** QUIN. **c** URB597. **d** URB597 + QUIN. Arrows denote living cells (preserved nuclei), and asterisks denote damaged cell nuclei. The right panel depicts the ratio of cell damage (damaged cells/total cells per field) from striatal tissue of animals exposed to QUIN and/or URB. Mean values ± SEM of $N = 4$–6 rats per group are represented. $^{+}P < 0.05$, different from Sham; two-way ANOVA followed by Tukey's test

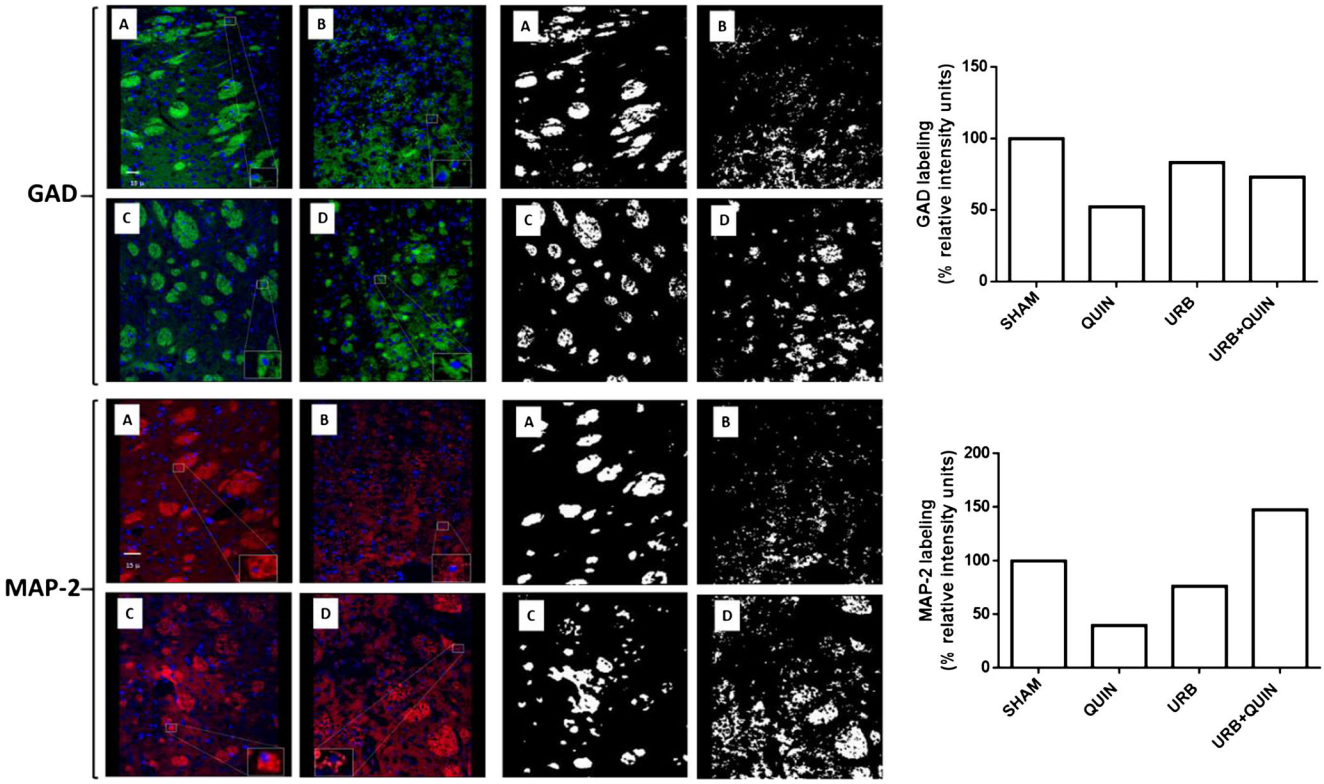

Fig. 4 Effects of quinolinic acid (QUIN) and/or URB597 (URB) on the striatal immunofluorescence labeling of neuronal (GABAergic) cells. The left panels show immunofluorescence photomicrographs (×20) of dorsal striatal coronal slices of animals exposed to QUIN and/or URB597. Immunofluorescence was directed against the GABAergic protein GAD (in green) and the neuronal protein MAP-2 (in red). **A** Sham. **B** QUIN, **C** URB597. **D** URB597 + QUIN. The most representative images collected from four rats (three sections of the dorsal striatum per rat) are depicted. Small squares show magnified details of immunopositive cells. Images of the same micrographs showing the segmentation process (contrasted labeling) are included (in black and white). The right panels depict the corresponding densitometric analysis obtained once the segmentation process was carried out. Bars in the graphs represent units of relative fluorescence intensity. No dispersion is represented as bars depict normalized mean values

patterns of GAD and MAP-2 (17 and 24% below the Sham group, respectively).

URB597 Prevented the QUIN-induced Striatal Lipid Peroxidation and Protein Carbonylation

Next, we measured the degree of early oxidative damage to lipids in striatal tissue samples of animals exposed to QUIN and/or URB597. The level of lipid peroxidation induced by QUIN was increased compared to the Sham group (974% above Sham, $P < 0.05$) as a response to the early toxic pattern elicited by QUIN (samples obtained at 24 h post-lesion; see Fig. 5, left panel). In contrast, URB597 prevented the toxic effect of QUIN in a significant manner (72% below QUIN group; $P < 0.05$). In turn, URB597 per se did not affect the striatal levels of lipid peroxidation compared to the Sham group.

The effects of QUIN and/or URB597 were also tested on the levels of protein carbonylation in striatal tissue samples. Figure 5 (right panel) shows that the average levels of protein carbonylation induced by QUIN after 24 h of exposure were significantly increased compared to the Sham group (94% above Sham; $P < 0.05$). In contrast, URB597 significantly reduced the QUIN-induced oxidative damage to proteins compared to the QUIN group (37% below QUIN; $P < 0.05$). URB597 per se did not affect the striatal levels of protein carbonylation compared to the Sham group.

QUIN and URB597 Modified the CB1 and NR1 Striatal Expression and Localization

Immunofluorescence against CB1 and NR1 proteins was evaluated in rat brain striatal coronal sections obtained 1.5 h post-lesion. Immunofluorescence assays were carried out to assess the distribution of the corresponding proteins within the stated time-lapse under the rationale that several intracellular events of toxic nature can take place in an early manner just during the first minutes of the excitotoxic insult; and compensatory and regulatory events triggered by URB597 could also occur during the first minutes of the excitotoxic insult, thus helping to explain neuroprotection.

Figure 6 depicts the images of nuclei stained with DAPI (in blue) merged with the CB1 or NR1 (both in red) staining. In the two upper lines of the micrographs (four left panels, ×20), the CB1 localization in the Sham group (A) appeared dotted,

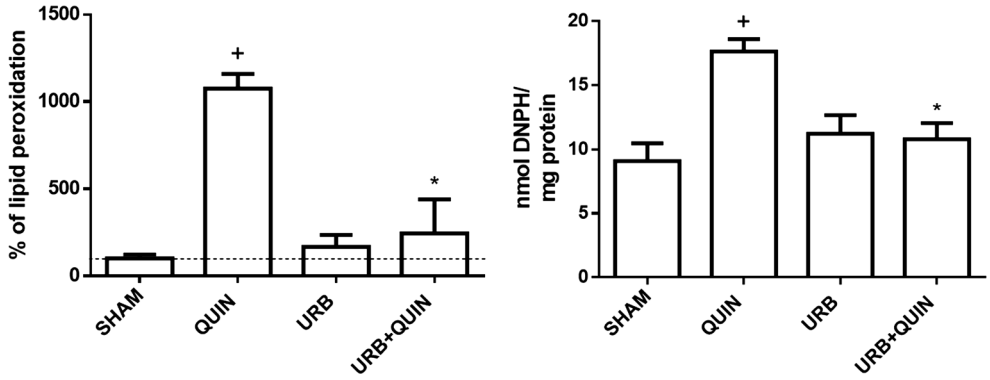

Fig. 5 Striatal levels of lipid peroxidation (percent of oxidative damage to lipids; left panel) and protein carbonylation (nmol DNPH/mg protein; right panel) of animals exposed to quinolinic acid (QUIN, for 24 h) and/or URB597 (URB). Mean values ± SEM of $N = 4–6$ rats per group are represented. $^{+}P < 0.05$, different from Sham, $^{*}P < 0.05$, different from QUIN; two-way ANOVA followed by Tukey's test

diffuse and mostly homogeneously distributed; in contrast, the QUIN lesion (B) produced a less dense localization remitted to some large spots of aggregation. In turn, URB597 per se (C) produced a denser and more aggregated distribution of CB1 in the striatal sections, whereas the URB597 + QUIN treatment (D) induced a decreased labeling for CB1 compared to the Sham group (similar to the QUIN group), being just remitted to some aggregated spots. These images were also contrasted using the segmentation imaging method, confirming the localization and distribution tendencies above described (four right panels).

In the two bottom lines of micrographs (four left panels, ×20), the NR1 localization in the Sham group (A) appeared homogeneously distributed and organized within striosomes. The QUIN treatment (B) also presented an organized localization of NR1 apparently remitted to some striosomes, but the

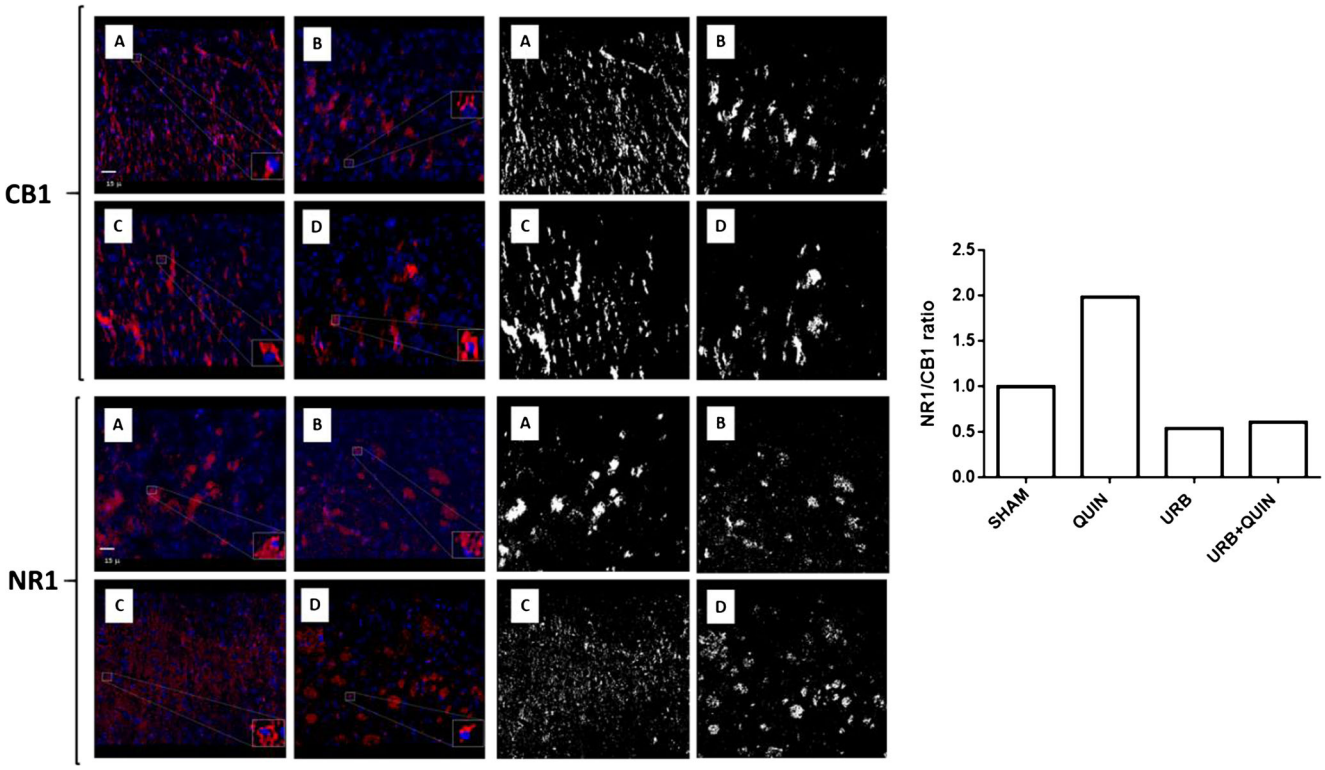

Fig. 6 Effects of URB597 (URB) and/or quinolinic acid (QUIN) on the immunofluorescence expression and localization of CB1 and NR1 in rat striatal tissue. DAPI staining in nuclei appears in blue; stained proteins appear in red for both cases (CB1 and Nr1). The most representative images collected from three rats (three sections of the dorsal striatum per rat) are depicted. In the upper composition (first two lines), immunofluorescence staining for CB1 is shown; in the bottom composition (third and fourth lines), the immunofluorescence staining for NR1 is depicted. In the eight panels from the left, the typical immunofluorescence signals are shown in coronal sections (×20); in the eight panels from the right, segmentation images contrasting real fluorescence signals are depicted. Small squares show magnified details of immunopositive cells. The intensity of the fluorescence signal was calculated using the ImageJ Software (version 1.47, NIH, Bethesda, Maryland, USA). Treatments in panels are as follows: **A** Sham, **B C** URB, and **D** URB + QUIN. In the graph appearing at the right side of the figure, the NR1/CB1 ratio in the dorsal striatum of rats from the different treatments is shown. No dispersion is represented as bars depict normalized mean values

staining was less dense (B) than that of the Sham group. URB597 per se (C) induced a less dense and more diffused distribution and localization of NR1 in the striatal sections, whereas the URB597 + QUIN treatment (D) induced a less intense labeling for NR1 compared to the Sham group (but still denser than the QUIN group), also preserving the localization of the protein mostly within striosomes. These images were also contrasted by the segmentation imaging method, confirming the localization and distribution tendencies above described (four right panels).

For each treatment, the average density of NR1 from several fields was contrasted with that of CB1 to obtain the NR1/CB1 ratio (bottom graph). Noteworthy, in contrast to the crude densities above described, QUIN increased the NR1/CB1 ratio by 98% above the Sham group (normalized to 1), whereas, URB597 and URB597 + QUIN treatments decreased this ratio by 50 and 46% below the Sham group, respectively.

Discussion

After the acknowledgement of the ECS as a lipid-signaling arrangement with physiological functions—such as motor coordination, immune responses or cognition, to name a few—this modulatory system is currently emerging as a significant target for therapeutic approaches under many pathological scenarios of diverse nature. Among the possible strategies behind these promising effects, the modulation of the ECS through both CB1 and CB2 with available agonists constitutes a frequent advance, but could also involve molecules altering the degrading process of endogenous cannabinoids. Considering this background, in this report, we have evaluated for the first time the protective role of URB597, a selective inhibitor of the FAAH, on the excitotoxic events elicited by QUIN in the rat striatum. For this purpose, several behavioral, morphological, and biochemical endpoints of toxicity were explored.

The toxic pattern exerted by QUIN comprised a significant decrease in the body weight gain, accompanied by an increase in the rotation behavior of rats induced after an apomorphine challenge. It has been demonstrated that the unilateral striatal lesion induced by the excitotoxic paradigm produced by QUIN in rats is responsible for the stimulation of an asymmetric behavior resulting from the severe damage to the striatal tissue [36]. Therefore, this endpoint clearly represents the degree of damage achieved after the toxic insult in animal models, which is produced by an unbalance of the neurotransmitter systems between the lesioned and the unlesioned hemispheres [37]. URB597 was able to prevent both the body weight loss and the motor asymmetry induced by QUIN, thus suggesting that the structural preservation of the striatal tissue due to the protective actions provided by this agent were sufficient to account for an adequate functioning of the physiological tasks regulated by the striatum, ultimately preserving the motor integrity. The protective properties of URB597 observed in this study are well supported by documented evidence demonstrating that this agent produces positive effects preventing body weight loss in rats in other neurotoxic models, including the one produced by the mitochondrial toxin 3-nitropropionic acid (3-NP) [22]. In addition, evidence demonstrating the capacity of URB597 to improve motor performance in rats subjected to neurotoxic insults has been reported recently. This evidence includes positive actions of this cannabinoid-profiled agent on the motor alterations (open field) induced by 3-NP and the Parkinsonian neurotoxin 6-hydroxydopamine (6-OHDA) in rats [22], as well as on motor deficits (open field) produced by the Parkinsonian neurotoxin 1-methyl-4-phenyl-1,2,3,6-tetrahydropyridine (MPTP) in mice [30].

Regarding the major morphological changes induced by QUIN in the striatum, the toxin produced pyknosis, vacuolation, and degraded neuropil. Similar effects have been reported in previous studies demonstrating the aggressiveness of the excitotoxic insult induced by QUIN [38]. It is assumed that the preservation of motor skills should be tightly related to the defense of the structural integrity of the striatum. As such, URB597 was able to protect the striatum against the toxic actions of QUIN, as evidenced by the conserved tissue appearance and the proportion of preserved cells. This effect was confirmed by the calculation of the cell damage ratio, which shows that the enhanced damage produced by QUIN was avoided by URB597. Supporting evidence of this neuroprotective capacity of URB597 has been recently reported for the toxic model induced by 3-NP and the morphological alterations generated by 6-OHDA in striatal and nigral tissues of rats [22].

To support a correlation between the behavioral (functional) and morphological (structural) preservation exerted by URB597 in the toxic paradigm induced by QUIN, it is pertinent to consider that, besides other contributing cells (glia), the cellular structure needing preferential protection is the neuronal cell type. The striatum has been shown to be enriched with medium-sized GABAergic neurons plenty of cortical glutamatergic innervations [39]; therefore, through the assessing of the expression and localization of the neuronal protein MAP-2 and the specific GABAergic marker GAD, we provided a precise approach to evidence specific neuronal protection. Here we found that the intensity and localization of the fluorescence labeling for these two proteins was decreased in the striatum of QUIN-exposed rats. Previous reports support these findings, as it has been shown that QUIN can reduce the MAP-2 labeling in cultured human neurons [40] and the GAD65 and GAD67 mRNA labeling in the rat striatum [41], thus validating these approaches as evidence of GABAergic neuronal damage in the toxic paradigm. In contrast to the effect of QUIN, URB597 partially preserved the labeling

and localization of both proteins, suggesting that the protective strategy displayed by this compound comprises the neuronal preservation. This concept is also supported by the functional (motor) conservation of the striatum from URB597 + QUIN-treated animals described above, as well as the neuroprotective actions already described for this agent in other neurotoxic models [22, 30].

As current indexes of oxidative stress, lipid peroxidation and protein carbonylation were estimated in the striatal tissue of rats subjected to the different treatments at 24 h post-lesion. We chose this time of evaluation to bring information on whether oxidative damage can be a causal event for the late morphological and behavioral compromise induced by QUIN. The toxin increased both the levels of lipid and protein oxidative damages, suggesting that early redox alterations could be an integral part of the excitotoxic pattern evoked by this toxic metabolite. Previous reports have demonstrated that these two markers are stimulated by QUIN at short times after its intrastriatal infusion [31, 42]. In fact, the production of hydroxyl radical and the consequent lipid peroxidation induced by this toxin can take only few minutes after its intrastriatal injection [43, 44], thus supporting the concept that oxidative stress, either linked to excitotoxicity or independent of NMDAr overactivation, contributes in a significant manner to the neurodegenerative events already in progress. Moreover, QUIN is capable of inducing significant changes in different critical antioxidant systems (both enzymatic and non-enzymatic) that are dependent on the cellular metabolism, subsequently contributing to cell damage via oxidative stress [22, 45]. In turn, URB597 prevented the QUIN-induced oxidative damage to lipids and proteins. This finding allows us to suggest three possible non-excluding scenarios for the protective effect of URB597: this molecule might reduce oxidative damage via FAAH inhibition and further AEA accumulation and CB1 activation [46], which in turn could indirectly regulate metabolic processes to reduce oxidative damage; URB597 could also exert an indirect effect through pathways not involving CB1 stimulation (to be demonstrated); in addition, URB597 might evoke a direct antioxidant effect as a possible free radical scavenger, as it has been shown that it can reduce the superoxide radical formation in a toxic model of ethanol intake [23] and decreases lipid peroxidation in other toxic models [22, 30]. In fact, the last scenario described is a property of URB597 deserving further investigation; in the meantime, this feature cannot be discarded as a key property of the protective pattern exerted by this molecule.

With the aim to characterize and identify a possible mechanism of protection induced by URB597 on the neurotoxicity evoked by QUIN, the immunofluorescence labeling for both CB1 and NR1 labeling was evaluated and quantified in the dorsal striata of animals from all treatments. QUIN altered the expression and localization patterns of CB1 and NR1 compared to the Sham group. Despite the decreased immunofluorescence labeling for NR1 induced by QUIN, the NR1/CB1 ratio—a more functional marker of the balance between these two receptors—denoted an overall increased expression of NR1 over CB1 in the striata of animals lesioned with the toxin, thus suggesting propitious conditions to trigger excitotoxic events. In this regard, it is necessary to consider that crude localization patterns of NR1 protein not necessarily reflect the functional status of the excitability induced by QUIN; instead, they could reflect an early compensatory effect to the persistent excitatory stimulation already in course, and/or an early reorganization of these receptors in preparation for the excitotoxic events to come. Noteworthy, URB597 given to QUIN-lesioned rats decreased the NR1/CB1 ratio, turning the balance of these two proteins more similar to the Sham condition, hence supporting the concept that these animals were less prompted to develop excitotoxic episodes. In turn, URB597 per se depleted the expression pattern of CB1, as expected. Therefore, though the NR1/CB1 ratio obtained from all experimental groups supports increased early excitotoxicity linked to CB1 deregulation and its prevention by URB597, through the preliminary data presented here, we cannot categorically confirm this mechanism until more detailed studies aimed to characterize the CB1 and NR1 regulation by URB595 can be performed. In a previous report, it was shown that CB1 mapping in the caudate-putamen of rats receiving QUIN was modified, as suggested by the in vivo receptor downregulation assessed through the [18F]MK-9470 uptake marker by PET [47]. This evidence supports the QUIN-induced alterations in the expression and localization patterns of CB1 seen in this study. Besides, it has been shown that the manipulation of the ECS through endogenous and synthetic CBr agonists can reduce the noxious events produced by the QUIN-evoked excitotoxicity. Our group has recently shown that the incubation of rat striatal primary cultured neurons and rat brain synaptosomal fractions with the endogenous AEA, and the synthetic CBr agonists WIN 55,212-2 and CP 55,940, all in the presence of QUIN, resulted in the prevention of different toxic endpoints in both biological preparations, including loss of cell viability, reduced immunolabeling for the neuronal marker Neu-N, and CB1, decreased mitochondrial function and oxidative damage [35]. Noteworthy, QUIN again demonstrated its capacity to decrease CB1, suggesting that this effect could be considered an early feature of excitotoxicity with potential causal implications. Indeed, the downregulation of CB1 in the human brain is a well-characterized hallmark of Huntington's disease (HD) patients [48] and has served to postulate this event as part of the degenerative processes taking place in the progression of the disease. As such, cannabinoid-based therapies are now under current investigation to improve different symptoms of HD patients [49].

Other groups have shown that the stimulation of the ECS results in efficient outcomes in the excitotoxic model induced

by QUIN. For instance, WIN55, 212-2 was shown to reduce the QUIN-induced increase in extracellular glutamate levels and attenuated the striatal damage through a mechanism that can be attributed to CB1 [50]. Experiments validating a protective role of a restricted population of CB1 located on glutamatergic terminals against excitotoxic insults were further reported [51]. Supporting evidence on the positive role of cannabinoid-profiled agents against QUIN toxicity was provided more recently with the use of the cannabigerol derivative VCE-003.2, a compound acting at the PPAR-gamma receptor [52]. VCE-003.2 attenuated the neuronal cell death induced by QUIN and reduced the mutant Huntingtin aggregates in striatal cells. Altogether, the evidence described above validates the exploration of compounds with different cannabinoid profiles to reduce excitotoxic insults linked to deleterious effects of the endogenous metabolite QUIN.

To this point, the main mechanism by which these compounds may exert neuroprotective actions is attributable to their properties to decrease neurotransmitter release at the presynaptic level and/or to reduce excitatory stimulation at the postsynaptic level. It has been demonstrated that the activation of CBr leads to a coupling of these receptors with NMDAr in a process accounting for neuroprotection in excitotoxic conditions via HINT1 protein regulation [25]. This interaction between receptors was better described as an ON:OFF switch composed by the σ1R-HINT1 complex, which controls G protein (GPCR)-NMDAr cross-regulation; among these proteins are cannabinoid receptors, and the complexing function may, in turn, be responsible for a reduction of NMDAr activity [53]. In addition, the relevance of this sophisticated ON:OFF switch system establishing the control exerted by CBr on NMDAr has been recently discussed and validated as a potential therapeutic mechanism at the experimental level [27]. We, therefore, hypothesize that URB597 might exert the protective effects observed in this study in part via AEA accumulation after inhibiting FAAH activity [54], with the subsequent regulation of these receptors. However, in light of other properties already reported for URB597, such as its antioxidant profile [22, 23, 30], we cannot discard a possible scenario for this molecule recruiting several other mechanisms to evoke integral protective responses against excitotoxic insults. While this scenario remains to be investigated in further studies, we suggest, in the meantime, that cannabinoid-based drugs designed to induce a physiological accumulation of endogenous CBr agonists at the experimental level are promising pharmacological tools to improve the clinical expectancies of patients coursing with excitotoxic episodes. A summary of the mechanisms hypothesized to occur in the protection exerted by URB597 in the QUIN toxic model is depicted in a schematic representation in Fig. 7.

Concluding Remarks

Results of this work demonstrate a neuroprotective effect of URB597 on different toxic events evoked by QUIN in the rat corpus striatum. These events comprised behavioral, morphological and biochemical markers of neurotoxicity that were prevented by URB597 with the apparent contribution of a potential reduction of excessive glutamatergic excitability. It is assumed then that URB597 may exert its actions in part via the inhibition of FAAH and the subsequent accumulation of

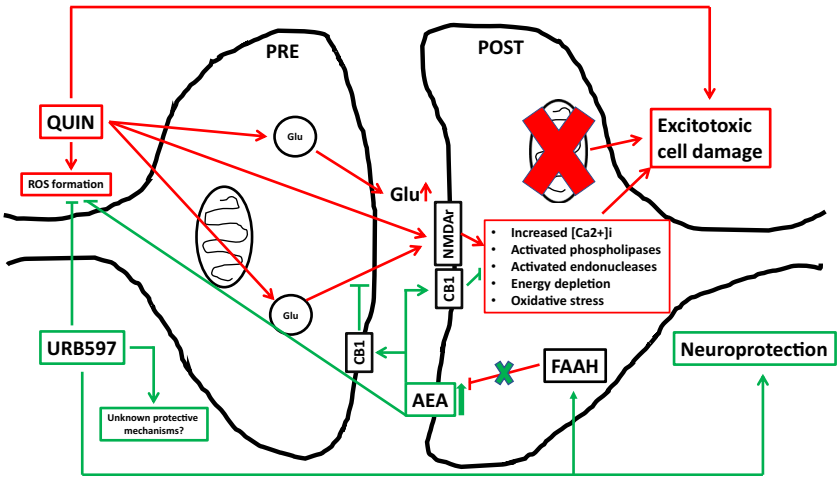

Fig. 7 Schematic representation of the events occurring at the synaptic level in the toxic model produced by quinolinic acid (QUIN) and the protective effects induced by the fatty acid amide hydrolase (FAAH) inhibitor URB597. The toxic actions of QUIN are mostly exerted via NMDAr overactivation, resulting in enhanced release of glutamate (Glu) at the presynaptic level, and increased intracellular Ca^{2+} levels and activation of deadly signaling cascades at the postsynaptic level that include energy depletion, reactive oxygen species (ROS) formation and oxidative stress, activation of endonucleases and phospholipases, etc. In contrast, URB597 might act at the following different levels: **a** induction of FAAH inhibition and further anandamide (AEA) accumulation with the subsequent stimulation of NMDAr control via CBr activation; **b** direct inhibition of oxidative stress induced by excitotoxicity; and **c** other mechanisms not yet identified. Red lines and frames symbolize toxic events; green lines and frames represent protective effects

endogenous AEA, thus possibly inducing the regulation of cannabinoid and glutamate receptors through mechanisms already described. However, since URB597 also possesses reported antioxidant activity per se, we cannot discard a possible involvement of this property in its neuroprotective pattern. URB597 is a promising pharmacological tool to explore biochemical and molecular mechanisms in neurodegenerative disease models, thus allowing the design of alternative therapies based on the manipulation of the ECS.

Acknowledgements Gabriela Aguilera-Portillo presents this article as the first author as it encompasses her work and efforts to obtain a Ph.D. degree at the Universidad Autónoma Metropolitana-Iztapalapa (Mexico). Authors express sincere gratitude to the Programa de Posgrado en Biología Experimental from the Universidad Autónoma Metropolitana-Iztapalapa for all the support provided throughout this study. We gratefully acknowledge the technical assistance of Dr. Ana Laura Colín-González. We also thank to the TUBITAK-SBAG (Project No.: 315S088).

Author Contributions GAP, AC, CK, IT, MK, and AS conceived and designed the experiments. GAP, ERL, JVH, GP, and AS performed the experiments and analyzed the data. GAP and AS wrote the paper. ÇK, ZE, AC, MK, GAP, and AS developed the theory and contributed to the final version of the manuscript.

Funding This work was supported by CONACyT-TUBITAK Grant 265991 (A.S.). Gabriela Aguilera-Portillo received a scholarship from CONACyT (CVU486539).

Compliance with Ethical Standards

Conflicts of Interest The authors declare that they have no competing interests.

Research Involving Animals Procedures carried out with animals were strictly developed to comply with the local guidelines for the use and care of laboratory animals (Norma Oficial Mexicana NOM-062-ZOO-2001), and the "Guidelines for the Use of Animals in Neuroscience Research" from the Society of Neuroscience. All experiments performed were timely approved by the Ethics Committee of the Instituto Nacional de Neurología y Neurocirugía. All efforts were made to minimize animal suffering during the experiments.

References

1. Zádori D, Klivényi P, Szalárdy L, Fülöp F, Toldi J, Vécsei L (2012) Mitochondrial disturbances, excitotoxicity, neuroinflammation and kynurenines: novel therapeutic strategies for neurodegenerative disorders. J Neurol Sci 322:187–191
2. Essa M, Braidy N, Vijayan K, Subash S, Guillemin G (2013) Excitotoxicity in the pathogenesis of autism. Neurotox Res J 23: 393–400
3. Iacobucci G, Popescu G (2017) NMDA receptors: linking physiological output to biophysical operation. Nat Rev Neurosci 18:236–249
4. Rami A, Ferger D, Krieglstein J (1997) Blockade of calpain proteolytic activity rescues neurons from glutamate excitotoxicity. Neurosci Res 27:93–97
5. Majewski M, Kozlowska A, Thoene M, Lepiarczyk E, Grzegorzewski W (2016) Overview of the role of vitamins and minerals on the kynurenine pathway in health and disease. J Physiol Pharmacol 67:3–19
6. Pérez-De La Cruz V, Konigsberg M, Santamaría A (2007) Kynurenine pathway and disease: an overview. CNS Neurol Disord Drug Targets 6:398–410
7. Ghorayeb I, Bezard E, Fernagut P, Bioulac B, Tison F (2005) Animal models of parkinsonism. Rev Neurol (Paris) 161:907–915
8. Ramaswamy S, McBride J, Kordower J (2007) Animal models of Huntington's disease. ILAR J 48:356–373
9. More S, Kumar H, Cho D, Yun Y, Choi D (2016) Toxin-induced experimental models of learning and memory impairment. Int J Mol Sci 17:E1447
10. Stone T, Mackay G, Forrest C, Clark C, Darlington L (2003) Tryptophan metabolites and brain disorders. Clin Chem Lab Med 41:852–859
11. Braidy N, Grant R, Adams S, Brew B, Guillemin G (2009) Mechanism for quinolinic acid cytotoxicity in human astrocytes and neurons. Neurotox Res J 16:77–86
12. Pérez-De La Cruz V, Elinos-Calderón D, Carrillo-Mora P, Silvia-Adaya D, Konigsberg M, Morán J, Ali S, Chánez-Cárdenas M et al (2010) Time-course correlation of early toxic events in three models of striatal damage: modulation by proteases inhibition. Neurochem Int 56:834–842
13. Howlett AC, Barth F, Bonner TI, Cabral G, Casellas P, Devane WA, Felder CC, Herkenham M et al (2002) International Union of Pharmacology. XXVII . Classification of cannabinoid receptors. Pharmacol Rev 54:161–202
14. Kendall D, Yudowski G (2016) Cannabinoid receptors in the central nervous system: their signaling and roles in disease. Front Cell Neurosci 10:294
15. Ashton J, Friberg D, Darlington C, Smith P (2006) Expression of the cannabinoid CB2 receptor in the rat cerebellum: an immunohistochemical study. Neuroscience 396:113–116
16. Lauckner J, Hille B, Mackie K (2005) The cannabinoid agonist WIN55,212-2 increases intracellular calcium via CB1 receptor coupling to Gq/11 G proteins. Proc Natl Acad Sci 102:19144–19149
17. Basavarajappa B, Shivakumar M, Joshi V, Subbanna S (2017) Endocannabinoid system in neurodegenerative disorders. J Neurochem 142:624–648
18. De Petrocellis L, Cascio M, Di Marzo V (2004) The endocannabionid system: a general view and latest additions. Br J Pharmacol 141:765–774
19. Palazuelos J, Aguado T, Pazos M, Julien B, Carrasco C, Resel E, Sagredo O, Benito C et al (2009) Microglial CB2 cannabinoid receptors are neuroprotective in Huntington's disease excitotoxicity. Brain 132:3152–3164
20. Fowler C (2006) The cannabinoid system and its pharmacological manipulation—a review, with emphasis upon the uptake and hydrolysis of anandamide. Fundam Clin Pharmacol 20(6):549–562
21. Hillard C, Jarrahian A (2003) Cellular accumulation of anandamide: consensus and controversy. Brain J Pharmacol 140:802–808
22. Maya-López M, Ruiz-Contreras H, de Jesús Negrete-Ruiz M, Martínez-Sánchez J, Benítez-Valenzuela J, Colín-González A, Villeda-Hernández J et al (2017) URB597 reduces biochemical, behavioral and morphological alterations in two neurotoxic models in rats. Biomed Pharmacother 88:745–753
23. Pelicao R, Santos M, Freitas-Lima L, Meyrelles S, Vasquez E, Nakamura-Palacios E, Rodrigues L (2016) URB597 inhibits oxidative stress induced by alcohol binging in the prefrontal cortex of adolescent rats. Neurosci Lett 15:17–22
24. Nazari M, Komaki A, Karamian R, Shahidi S, Sarihi A, Asadbegi M (2016) The interactive role of CB1 and GABA B receptors in hippocampal synaptic plasticity in rats. Brain Res Bull 120:123–130

25. Sánchez-Blázquez P, Rodríguez-Muñoz M, Vicente-Sánchez A, Garzón J (2013) Cannabinoid receptors couple to NMDA receptors to reduce the production of NO and the mobilization of zinc induced by glutamate. Antioxid Redox Signal 19(15):1766–1782
26. Sánchez-Blázquez P, Rodríguez-Muñóz M, Garzón J (2014) The cannabinoid receptor 1 associates with NMDA receptors to produce glutamatergic hypofunction: implications in psychosis and schizophrenia. Front Pharmacol 4:169
27. Rodríguez-Muños M, Sánchez-Blázquez P, Merlos M, Garzón-Niño J (2016) Endocannabinoid control of glutamate NMDA receptors: the therapeutic potential and consequences of dysfunction. Oncotarget 34:55840–55862
28. O'Sullivan S (2007) Cannabinoids go nuclear: evidence for activation of peroxisome proliferator-activated receptors. Br J Pharmacol 152:576–582
29. O'Sullivan S (2016) An update on PPAR activation by cannabinoids. Br J Pharmacol 12:1899–1910
30. Escamilla-Ramírez A, García E, Palencia-Hernández G, Colín-González A, Galván-Arzate S, Túnez I, Sotelo J, Santamaría A (2017) URB597 and the cannabinoid WIN55,212-2 reduce behavioral and neurochemical deficits induced by MPTP in mice: possible role of redox modulation and NMDA receptors. Neurotox Res 34:532–544
31. Colín-González A, Orozco-Ibarra M, Chánez-Cárdenas M, Rangel-López E, Santamaría A, Pedraza-Chaverri J, Barrera-Oviedo D, Maldonado P (2013) Heme oxygenase-1 (HO-1) upregulation delays morphological and oxidative damage induced in an excitotoxic/pro-oxidabt model in the rat striatum. Neuroscience 12:91–101
32. Paxinos G, Watson C (1998) The rat brain in stereotaxic coordinates, 4th ed. Academic Press
33. Borlongan C, Randall T, Cahill D, Sanberg P (1995) Asymmetrical motor behavior in rats with unilateral striatal excitotoxic lesions as revealed by the elevated body swing test. Brain Res 676:231–234
34. González R, Woods R (2008) Digital image processing, 3rd edn. Pearson Prentice Hall, USA
35. Rangel-López E, Colín-González A, Paz-Loyola A, Pinzón E, Torres I, Serratos I, Castellanos P, Wajner M et al (2015) Cannabinoid receptor agonists reduce the short-term mitochondrial dysfunction and oxidative stress linked to excitotoxicity in the rat brain. Neuroscience 285:97–106
36. Dunbar J, Hitchcock K, Latimer M, Rugg E, Ward N, Winn P (1992) Exctitotoxic lesions of the pedunculopontine tegmental nucleus of the rat. II. Examination of eating and drinking, rotation, and reaching and grasping following unilateral ibotenate of quinolinate lesions. Brain Res 589:194–206
37. Trigo-Damas I, Del Rey N, Blesa J (2018) Novel models for Parkinson's disease and their impact on future drug discovery. Expert Opin Drug Discovery 13:229–239
38. Santamaría A, Salvatierra-Sánchez R, Vázquez-Román B, Santiago-López D, Villeda-Hernández J, Galván-Arzate S, Jiménez-Capdeville M et al (2003) Protective effects of the antioxidant selenium on quinolinic acid-induced neurotoxicity in rats: In vitro and in vivo studies. J Neurochem 86: 479–488
39. Holley S, Joshi P, Parievsky A, Galvan L, Chen J, Fisher Y, Huynh M, Cepeda C et al (2015) Enhanced GABAergic inputs contribute to functional alterations of cholinergic interneurons in the R6/2 mouse model of Huntington's disease. eNeuro 2:e0008
40. Kerr S, Armati P, Guillemin G, Brew B (1998) Chronic exposure of human neurons to quinolonic acid results in neuronal changes consistent with AIDS dementia complex. AIDS 5:355–363
41. Qin Y, Soghomonian J, Chesselet M (1992) Effects of quinolinic acid on messenger RNAs encoding somatostatin and glutamic acid decarboxylases in the striatum of adult rats. Exp Neurol 115:200–211
42. Santana-Martínez R, Galván-Arzáte S, Hernández-Pando R, Chánez-Cárdenaz M, Avila-Chávez E, López-Acosta G, Pedraza-Chaverrí J, Santamaría A et al (2014) Sulphoraphane reduces the alterations induced by quinolinic acid: Modulation of glutathione levels. Neuroscience 272:188–198
43. Rios C, Santamaría A (1991) Quinolinic acid is a potent lipid peroxidant in rat brain homogenates. Neurochem Res 16:1139–1143
44. Santamaría A, Galván-Arzate S, Lisý V, Ali S, Duhart H, Osorio-Rico L, Ríos C, St'astný F (2001) Quinolinic acid induces oxidative stress in rat brain synaptosomes. Neuroreport 12:871–874
45. Rodríguez-Martínez E, Camacho A, Maldonado P, Pedraza-Chaverrí J, Santamaría D, Galván-Arzate S, Santamaría A (2000) Effect of quinolinic acid on endogenous antioxidants in rat corpus striatum. Brain Res 858:436–439
46. Howlett A, Abood M (2017) CB1 and CB2 receptor pharmacology. Adv Pharmacol 80:169–206
47. Casteels C, Martinez E, Bormans G, Camon L, de Vera N, Baekelandt V, Planas A, Laere K (2010) Type 1 cannabinoid receptor mapping with [18F]MK-9470 PET in the rat brain after quinolinic acid lesion: a comparison to dopamine receptors and glucose metabolism. Eur J Nucl Med Mol Imaging 37:2354–2363
48. Dowie M, Howard M, Nicholson L, Faull R, Hannan A, Glass M (2010) Behavioural and molecular consequences of chronic cannabinoid treatment in Huntington's disease transgenic mice. Neuroscience 170:324–336
49. Sagredo O, Pazos M, Valdeolivas S, Fernández-Ruiz J (2012) Cannabinoids: novel medicines for the treatment of Huntington's disease. Recent Patents CNS Drug Discov 7:41–48
50. Pintor A, Tebano M, Martire A, Grieco R, Galluzzo M, Scattoni M, Pézzola A, Cocurello R et al (2006) The cannabinoid receptor agonists WIN 55,212-2 attenuates the effects induced by quinolinic acid in the rat striatum. Neuropharmacology 51:1004–1012
51. Chiarlone A, Bellocchio L, Blázquez C, Resel E, Soria-Gómez E, Cannich A, Ferrero J, Sagredo O et al (2014) A restricted population of CB1 cannabinoid receptors with neuroprotective activity. Proc Natl Acad Sci Press 111:8257–8262
52. Diaz-Alonso J, Paraíso-Luna J, Navarrete C, del Rïo C, Cantarero I, Palomares B, Aguareles J, Fernández-Ruiz J et al (2016) VCE-003.2, a novel cannabigerol derivative, enhances neuronal progenitor cell survival and alleviates symptomatology in murine models of Huntington's disease. Sci Rep 6:29789
53. Rodríguez-Muñoz M, Cortés-Montero E, Pozo-Rodrigálvarez A, Sánchez-Blázquez P, Garzón-Niño J (2015) The ON:OFF switch, σ1R-HINT1 protein, controls GPCR-NMDA receptor cross-regulation: Implications in neurological disorders. Oncotarget 6:35458–35477
54. Panlilio LV, Justinova Z, Goldberg SR (2010) Animal models of cannabinoid reward. Br J Pharmacol 160:499–510